THE JOURNAL OF BIOLOGICAL CHEMISTRY VOL. 287, NO. 21, pp. 17029–17039, May 18, 2012
Published in the U.S.A.

Selective Gα_i Subunits as Novel Direct Activators of Transient Receptor Potential Canonical (TRPC)4 and TRPC5 Channels*[S]

Received for publication, November 22, 2011, and in revised form, March 26, 2012 Published, JBC Papers in Press, March 28, 2012, DOI 10.1074/jbc.M111.326553

Jae-Pyo Jeon[‡1,2], Chansik Hong[‡1,2], Eun Jung Park[‡2], Ju-Hong Jeon[‡], Nam-Hyuk Cho[§], In-Gyu Kim[¶], Han Choe[‖], Shmuel Muallem[**], Hyun Jin Kim[‡‡3], and Insuk So[‡4]

*From the [‡]Department of Physiology, Seoul National University College of Medicine, Seoul 110-799, Korea, the [§]Department of Microbiology and Immunology, Seoul National University College of Medicine, Seoul 110-799, Korea, the [¶]Department of Biochemistry, Seoul National University College of Medicine, Seoul 110-799, Korea, the [‖]Department of Physiology, University of Ulsan College of Medicine, Seoul 136-748, Korea, the **Epithelial Signaling and Transport Section, Molecular Physiology and Therapeutics Branch, NIDCR, National Institutes of Health, Bethesda, Maryland 20892, and the [‡‡]Department of Physiology, Sungkyunkwan University School of Medicine, Suwon 440-746, Korea*

Background: Activation of TRPC4/5 channels is mediated by GPCR activation.
Results: TRPC4/5 was activated by the G$\alpha_{i/o}$-coupled receptor and the Gα_i protein, which interacted directly with each other.
Conclusion: Gα_i proteins play an essential role as novel activators of TRPC4/5.
Significance: Our findings provide new insights into the activation mechanism of inhibitory Gα proteins.

The ubiquitous transient receptor potential canonical (TRPC) channels function as non-selective, Ca^{2+}-permeable channels and mediate numerous cellular functions. It is commonly assumed that TRPC channels are activated by stimulation of Gα_q-PLC-coupled receptors. However, whether the Gα_q-PLC pathway is the main regulator of TRPC4/5 channels and how other Gα proteins may regulate these channels are poorly understood. We previously reported that TRPC4/TRPC5 can be activated by Gα_i. In the current work, we found that Gα_i subunits, rather than Gα_q, are the primary and direct activators of TRPC4 and TRPC5. We report a novel molecular mechanism in which TRPC4 is activated by several Gα_i subunits, most prominently by Gα_{i2}, and TRPC5 is activated primarily by Gα_{i3}. Activation of Gα_i by the muscarinic M2 receptors or expression of the constitutively active Gα_i mutants equally and fully activates the channels. Moreover, both TRPC4 and TRPC5 are activated by direct interaction of their conserved C-terminal SESTD (SEC14-like and spectrin-type domains) with the Gα_i subunits. Two amino acids (lysine 715 and arginine 716) of the TRPC4 C terminus were identified by structural modeling as mediating the interaction with Gα_{i2}. These findings indicate an essential role of Gα_i proteins as novel activators for TRPC4/5 and reveal the molecular mechanism by which G-proteins activate the channels.

Transient receptor potential canonical (TRPC)[5] channels are considered the molecular candidates for receptor-operated Ca^{2+}-permeable cation channels. The G-protein-coupled receptor (GPCR)-Gα_q-PLC is assumed to be the primary pathway for activation of all TRPC channels, even though the exact mechanism by which the channels are activated remains unknown (1). Several mediators have been proposed to mediate channel activation by stimulation of GPCR. Among them are SESTD1 (2), intracellular Ca^{2+} (3, 4), lipid metabolites (5, 6), PIP_2 (7–9), calmodulin (10, 11), CaM kinase (12), MLCK (13–15), and channel exocytosis (16). In addition, TRPC4 and TRPC5 can be activated by thioredoxin (17) and NO (18).

The physiological role of these channels was established recently, demonstrating that TRPC4 and TRPC6 are the molecular candidates for the non-selective cation channels activated by muscarinic receptor stimulation (mI_{CAT}) in visceral smooth muscle cells. mI_{CAT} mediates the physiological action of acetylcholine in evoking smooth muscle contraction (19). Activation of muscarinic receptors causes the opening of non-selective cationic channels in smooth muscle cells of the gastrointestinal tract (20, 21). In these cells, PTX-sensitive G-proteins but not G$\beta\gamma$ were suggested to mediate channel activation (22, 23). At the level of M2 or M3 muscarinic receptors, Sakamoto *et al.* (24) showed three distinct signaling pathways that activate cationic channels in murine gut smooth muscle cells. The three pathways include the M2, M3, and M2/M3 pathways and were demonstrated using M2 KO, M3 KO, and M2/M3 double KO mice, respectively. In addition, the M2/M3 pathway but not the M2 or M3 pathways involves processes in which Ca^{2+} has a potentiating effect on channel activation, suggesting that the M3 pathway may facilitate the function of the M2/M3 pathway

* This work was supported by the National Research Foundation of Korea funded by the Ministry of Education, Science and Technology (MEST) (2008-2005948 and 2010-0019472).
[S] This article contains supplemental Figs. S1–S6.
[1] Both authors contributed equally to this work.
[2] Supported by the graduate program of the BK21 project from MEST.
[3] To whom correspondence may be addressed: Dept. of Physiology, Sungkyunkwan, University School of Medicine, Suwon 440-746, Korea. Tel.: 82-31-299-6105; Fax: 82-2-299-6129; E-mail: kimhyunjin@skku.edu.
[4] To whom correspondence may be addressed: Dept. of Physiology, Seoul National University, College of Medicine, Seoul 110-799, Korea. Tel.: 82-2-740-8228; Fax: 82-2-763-9667; E-mail: insuk@snu.ac.kr.

[5] The abbreviations used are: TRPC, transient receptor potential canonical; GPCR, G-protein-coupled receptor; EGFP, enhanced GFP; GTPγS, guanosine 5′-3-*O*-(thio)triphosphate; PTX, pertussis toxin; BAPTA, 1,2-bis(o-aminophenoxy)ethane-*N*,*N*,*N*′,*N*′-tetraacetic acid; PIP_2, phosphatidylinositol 4,5-bisphosphate; CaMK, Ca^{2+}/calmodulin-dependent protein kinase; PLC, phospholipase C; GI, gastrointestinal; pS, picosiemen; n.s., not significant; N.B., non-buffered.

through inositol 1,4,5-trisphosphate-induced Ca^{2+} release (24). Similarly, activation of mI_{CAT} requires the simultaneous activation of both the M2 and M3 muscarinic receptors (20), further suggesting involvement of $G\alpha_i$ in channel activation.

Several studies have also suggested that PTX-sensitive G-proteins play an important role in the activation process of TRPC4 and TRPC5 by GPCR (6, 8, 25). In our previous study, we showed that $G\alpha_{i2}$ activates TRPC4β and that PTX inhibits the activation of TRPC4β by stimulation of M2 muscarinic receptors (25). However, the specificity for $G\alpha_i$ subunits and how the PTX-sensitive G-proteins activate the channels are not yet known; it is assumed that the PTX-sensitive G-proteins activate the channels by an indirect mechanism that involves the generation of second messengers. The well known second messenger of PTX-sensitive G-proteins is cyclic AMP (cAMP), found downstream of adenylate cyclase. PTX-sensitive G-proteins inhibit adenylate cyclase, which in turn decreases cAMP concentration. In our recent study, we showed that cAMP inhibits TRPC4 and TRPC5 currents by activating PKA and phosphorylating TRPC4 and TRPC5 channels (26). Thus, it cannot be the mechanism by which $G\alpha_i$ activates the channels.

These findings prompted us to ask whether TRPC4 and TRPC5 are activated by other PTX-sensitive $G\alpha_{i/o}$ subunits and whether the activation is direct. We were also interested in identifying the TRPC4/5 domain that mediates the interaction with the channels and the activation by $G\alpha_{i/o}$ subunits, as well as the roles $G\alpha_q$ plays in modulating TRPC4/5. In the present study, we focused on the role of $G\alpha_i$ proteins in regulating TRPC4/5 and report that $G\alpha_i$ subunits specifically activate TRPC4 and TRPC5 by direct interaction with the channels. Moreover, the regulation is specific to $G\alpha_i$ subunits. TRPC4 is mainly activated by $G\alpha_{i2}$, whereas TRPC5 is primarily activated by $G\alpha_{i3}$. These findings explain how TRPC4 is activated to regulate GI motility. Strategies can now be developed to understand the functional consequences of activation of TRPC4/5 in the central and peripheral nervous systems.

EXPERIMENTAL PROCEDURES

Cell Culture and Transient Transfection, cDNA Clones—Human embryonic kidney (HEK293) cells (ATCC, Manassas, VA) were maintained according to the supplier's recommendations. For transient transfection, cells were seeded in 12-well plates. The following day, 0.5 μg/well of pcDNA3 vector containing the cDNA for mouse TRPC4β was mixed with 50–100 ng/well of pEGFP-N1 (Clontech) and transfected using the transfection reagent FuGENE 6 (Roche Molecular Biochemicals), as detailed in the manufacturer's protocol. Human TRPC5-EGFP cDNA and mouse TRPC4β-EGFP cDNA were also transfected in the same way. Coexpression of TRPC channels with G-proteins or receptors was achieved through a channel to G-protein transfection ratio of 1:1. After 30–40 h, the cells were trypsinized and transferred to a small recording chamber (RC-11, Warner Instruments) for whole-cell recording. HEK293 cells stably expressing mouse TRPC4β were established by G418 selection. The cells were cultured as for the transient transfection, except that the medium was supplemented with G418 (400 μg/ml). Human $G\alpha_{i1}^{Q204L}$, $G\alpha_{i2}^{Q205L}$, $G\alpha_{i3}^{Q204L}$, rat $G\alpha_{i2}^{Q205L}$, and human $G\alpha_q^{Q209L}$ were cloned into pcDNA3.1+. Human $G\beta_1$, $G\beta_2$, $G\beta_3$, $G\beta_5$, and bovine $G\gamma_2$ were cloned into pcDNA3.1+ (Invitrogen). Human $G\alpha_{oA}^{Q205L}$, M2 receptor (the Missouri S&T cDNA Resource Center), and M3 receptor were cloned into pcDNA3.1+. Human $G\beta_1$ was used to insert the $G\beta_1^{W99A}$ and $G\beta_1^{I80A}$ mutations using the QuikChange site-directed mutagenesis kit (Stratagene).

Western Blotting and Co-immunoprecipitation—Transfected cells were collected and lysed using 300 μl of binding buffer (50 mM HEPES, pH 7.4, 120 mM NaCl, 2 mM EDTA, 2 mM $MgCl_2$, complete protease inhibitor mixture tablet, phosphatase inhibitor mixture tablet (Roche Applied Science), and 0.5% Triton X-100). The lysates were sonicated, and any insoluble material was removed by centrifugation at 13,300 $\times$ *g* for 10 min. For co-immunoprecipitation of TRPC4β-GFP and TRPC5-GFP with $G\alpha_{i2}$ and $G\alpha_{i3}$, anti-GFP antibody (1 μg, Invitrogen, A11122) was added to 100 μl cell extract and incubated for 12 h at 4 °C. Then, 50 μl of a 1:1 slurry of protein G-Sepharose 4B beads was added to the antibody-extract mix and incubated for 12 h at 4 °C. Beads were washed three times with binding buffer; proteins were released from the beads with 50 μl of 2× SDS-loading buffer and analyzed with 10% or 8% SDS-PAGE. $G\alpha_{i2}$ and $G\alpha_{i3}$ were co-precipitated with GFP antibody and probed by mouse monoclonal anti-$G\alpha_{i2}$ antibody (2 μg, Santa Cruz Biotechnology, sc-13534) and mouse monoclonal anti-EE antibody for $G\alpha_{i3}$ (2 μg, Covance, MMS-115P). The mouse monoclonal anti-$G\alpha_{i2}$ antibody was used for a reciprocal co-immunoprecipitation with GFP antibody in a sequential experiment. Co-immunoprecipitation of TRPC4β-GFP with $G\alpha_q$ was achieved using the same procedures. $G\alpha_q$ was probed by mouse monoclonal anti-$G\alpha_q$ antibody (Santa Cruz Biotechnology, sc-136181).

Rat brain from day 15 was homogenized on ice using a Dounce homogenizer. The homogenate buffer had the same composition as the binding buffer. Homogenates were centrifuged at 13,000 rpm for 30 min at 4 °C. Supernatants were re-centrifuged at 13,000 rpm at 4 °C for 20 min. Supernatants were pre-cleared with protein G-Sepharose beads for 1 h at 4 °C and centrifuged at 2000 rpm for 2 min at 4 °C. Fifty microliters of a 1:1 slurry of protein G-Sepharose beads was added to the rabbit polyclonal antibody (anti-$G\alpha_{i2}$, Santa Cruz Biotechnology, sc-7276 and anti-$G\alpha_{i3}$, Santa Cruz Biotechnology, sc-262) extract mix and incubated for 12 h at 4 °C. The omission of primary antibody was used as a control. Beads were washed three times with binding buffer. Immunoprecipitated proteins were probed with anti-TRPC4 (NeuroMab, 75–119) and anti-TRPC5 (NeuroMab, 75–104) on an 8% SDS-PAGE gel. Anti-TRPC4 and Anti-TRPC5 were used for reciprocal pulldowns. Controls were omission of the primary antibody and substitution of normal anti-mouse IgG with non-immune serum (Santa Cruz Biotechnology, sc-2025). Rabbit polyclonal anti-$G\alpha_{i2}$ (2 μg, Santa Cruz Biotechnology) and rabbit polyclonal anti-$G\alpha_{i3}$ (2 μg, Santa Cruz Biotechnology) antibodies were used to probe co-immunoprecipitation samples on a 10% SDS-PAGE gel.

Surface Biotinylation—Cells were washed with and suspended in PBS. Suspended cells were incubated in 0.5 mg/ml sulfo-NHS-LC-biotin (Pierce) in PBS for 30 min on ice. Free biotin was quenched by the addition of 100 mM glycine in PBS. Lysates were prepared in lysis buffer by being passed 7–10 times

through a 26-gauge needle after sonication. Lysates were centrifuged at 13,300 × *g* for 10 min at 4 °C, and protein concentrations of the supernatants were determined. Forty microliters of a 50% slurry of avidin beads (Pierce) was added to cell lysates equivalent to 400 μg of protein. After incubation for 1 h at room temperature, beads were washed three times with 0.5% Triton X-100 in PBS, and proteins were extracted in sample buffer. Collected proteins were then analyzed by 8% SDS-PAGE gel and probed by anti-GFP antibody (Invitrogen, A11122).

GST Pulldown Assays—The C-terminal domain of TRPC4-(621–890) was cloned into BamHI-SalI restriction sites of pGEX4T-1 (Amersham Biosciences Pharmacia) by PCR. The GST fusion constructs were expressed and purified from *Escherichia coli* (BL21(DE3)). Briefly, *E. coli* were grown in liquid cultures containing 0.1 mM isopropyl 1-thio-β-D-galactopyranoside with vigorous agitation for 18 h at 20 °C to an A_{600} of 0.6. Channel protein was purified from the soluble extract using glutathione-agarose beads (Amersham Biosciences). GST fusion proteins appeared to be sensitive to degradation and carefully utilized in subsequent binding assays conducted within 24 h following purification. Histidine-tagged $G\alpha_{i2}{}^{Q205L}$ protein was expressed in *E. coli* (BL21(DE3)) from the pET15b plasmid containing full-length human $G\alpha_{i2}{}^{Q205L}$ cDNA. Histidine-tagged forms of $G\alpha_{i2}{}^{Q205L}$ were purified using immobilized Ni^{2+}-nitrilotriacetic acid affinity chromatography. Binding between $G\alpha_{i2}{}^{Q205L}$ and the GST fusion C-terminal domain of TRPC4 was allowed to occur for 1 h at room temperature on a plate rotator. Each reaction sample was subsequently centrifuged at 500 × *g* for 5 min. After three washes with 500 μl of PBS with 0.1% Triton X-100, the GST protein-G-protein complexes were eluted with 15 μl of 2× SDS sample buffer, and the entire sample was run on a 10% polyacrylamide-SDS gel. Mouse monoclonal anti-$G\alpha_{i2}$ (Santa Cruz Biotechnology) and anti-GST antibodies (Santa Cruz Biotechnology, sc-138) were used for immunoblot analyses. Unless otherwise stated, all pulldown assays were repeated three times for each condition.

Whole-cell Patch Clamp Experiment—The whole-cell configuration was used to measure TRPC channel current in HEK cells as described previously (13, 19, 23, 27). Cells were transferred to a small chamber on the stage of an inverted microscope (TE2000S, Nikon Japan), and attached to coverslips in the small chamber for 10 min prior to patch recording. Currents were recorded using an Axopatch 200B patch clamp amplifier (Axon Instrument). Bath solutions were constantly perfused with a physiological salt solution at a rate of 1–2 ml/min. Glass microelectrodes with 2–4 megohm resistance were used to obtain gigaohm seals. After establishing the whole-cell configuration, the external solution was changed from Normal Tyrode to Cs^+-rich external solution. The current was recorded in 500-ms duration RAMPs from +100 to −100 mV and from a holding membrane potential of −60 mV. pCLAMP software (version 10.2) and Digidata 1440A (Axon Instruments) were used for data acquisition and application of command pulses. Data were filtered at 5 kHz and displayed on a computer monitor. Data were analyzed using pCLAMP (version 10.2) and Origin software (Microcal origin, version 7.5).

Solutions and Drugs—For all TRPC channel recordings, physiological salt solution containing 135 mM NaCl, 5 mM KCl, 2 mM $CaCl_2$, 1 mM $MgCl_2$, 10 mM glucose, and 10 mM HEPES. The pH was adjusted to 7.4 using NaOH. Cs^+-rich external solution was prepared by replacing NaCl and KCl with equimolar CsCl. The pipette solution contained 140 mM CsCl, 10 mM HEPES, 0.2 mM Tris-GTP, 0.5 mM EGTA, and 3 mM Mg-ATP. The pH was adjusted to 7.3 with CsOH. Pertussis toxin was purchased from Calbiochem (La Jolla, CA), and carbachol, HEPES, and GTPγS were purchased from Sigma.

Modeling of Interaction Between $G\alpha_{i2}$ and TRPC4—The homology model of $G\alpha_{i2}$ structure was constructed using MODELLER 9v8 (28) based on two Gα structures that have high sequence homology with $G\alpha_{i2}$ (Protein Data Bank codes 2ODE and 1GP2). Due to the absence of a known protein structure homologous to TRPC4, the structure of TRPC4 C terminus was modeled using I-TASSER, which combines the methods of threading, *ab initio* modeling, and structural refinement (29, 30). The docking of the TRPC4 C terminus on the $G\alpha_{i2}$ was initiated because the putative binding site of TRPC4 (amino acids 701–720) contains positive charges conserved among TRPC channels. An ionic interaction was assumed between the sites of the mTRPC4 and $G\alpha_{i2}$. There are nine sites where the $G\alpha_i$ family has negative charges, but the $G\alpha_{q/11}$ family does not. Seven crystal structures of protein complexes between Gα and other proteins (Protein Data Bank codes 2RGN, 2ODE, 3CX6, 2G83, 1FQJ, 2BCJ, and 1GP2) were inspected visually, and it was found that only specific areas of Gα participated in interactions with other proteins. Therefore, manual docking was carried out between $G\alpha_{i2}$ and the TRPC4 C terminus, emphasizing the close interaction between the two conserved positive charges of TRPC4, Arg-711 and Lys-715, and the conserved positive charges of $G\alpha_{i2}$, Asp-252.

Statistics—All data are expressed as means ± S.E. Statistical significance was determined using paired or unpaired Student's *t* tests. *p* values of < 0.05 were considered statistically significant. The number of cell recordings is represented by *n*.

RESULTS

Expression of TRPC4 alone results in a minimal spontaneous current (2.1 ± 1.1 pA/pF; see Fig. 2*B*, mock, open column, $n = 5$), compared with TRPC5, which showed a significant basal current (Fig. 2*C*, 36.6 ± 9.2 pA/pF, $n = 14$; see also Ref. 26). Although HEK cells endogenously express muscarinic receptors, most likely the M3 subtype (31), the endogenous receptors do not activate TRPC4 (Fig. 1*B*, mock) (32). In the case of TRPC5, the endogenous muscarinic receptor elicited only small transient TRPC5 activation. Therefore, we analyzed the TRPC4 and TRPC5 currents induced by heterologously expressed muscarinic receptors or by intracellular infusion of GTPγS through the patch pipette. The TRPC maximal inward currents (in Cs^+-rich solution) at negative membrane potentials (−60 mV) are represented as a current density (pA/pF). In all cases, maximal peak inward currents were obtained by subtracting the current recorded in bath Cs^+.

Muscarinic Receptor Stimulation Activates TRPC4 and TRPC5 through Endogenous $G\alpha_{i/o}$—First, we tested the effects of the expressed $G\alpha_i$-coupled M2 and the $G\alpha_q$-coupled M3 muscarinic receptors on the activation of TRPC4 or TRPC5 by endogenous G-proteins in HEK cells (Fig. 1). Activation of the

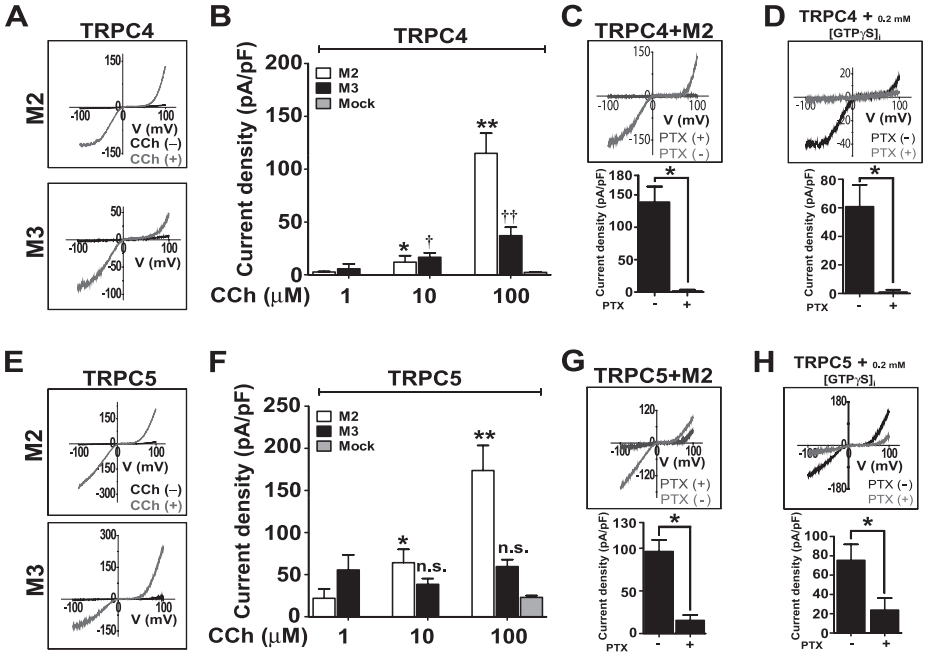

FIGURE 1. **Activation of endogenous G$\alpha_{i/o}$ by the muscarinic M2 receptor activates TRPC4 and TRPC5.** *A*, carbachol (*CCh*) activated-TRPC4 current was recorded in HEK cells expressing TRPC4 and either M2 and M3 receptors. The representative *I-V* relationships of M2- and M3-evoked TRPC4 currents by 100 μM carbachol were recorded by voltage RAMPS of +100 to −100 mV during 500-ms durations, whereas the cells were held at −60 mV. *B* summarizes the amplitude of M2- and M3-activated TRPC4 currents activated by 1–100 μM carbachol. Current density is represented by maximal current peaks (subtracted Cs^+ basal current) at −60 mV in Cs^+ solution (changed from Normal Tyrode, Na^+) and is indicated by means ± S.E. Statistical significance was denoted by an *asterisk* (*open column*, 1 μM *versus* 10 μM) and *double asterisk* (*open column*, 10 μM *versus* 100 μM), *single dagger* (*closed column*, 1 μM *versus* 10 μM) and *double dagger* (*closed column*, 10 μM *versus* 10 μM) at $p < 0.05$. *C* and *D*, *I-V* relationship and current densities of M2- and GTPγS-evoked TRPC4 currents show inhibition by PTX pretreatment (100 ng/ml for 16 h). Statistical significance was denoted by an *asterisk* ($p < 0.05$). *E*, the representative *I-V* relationships of M2- and M3-activated TRPC5 currents were measured in cells stimulated with 100 μM carbachol. *F*, summary of the M2-activated TRPC5 current at 1–100 μM carbachol. Current density was obtained by the methods described above. Statistical significance was denoted by an *asterisk* (*open column*, 1 μM *versus* 10 μM) and *double asterisk* (*open column*, 10 μM *versus* 100 μM) at $p < 0.05$. *G* and *H*, the representative *I-V* relationships and current densities of M2- and GTPγS-evoked TRPC5 currents show inhibition by PTX pretreatment (as described under "Experimental Procedures"). Statistical significance was denoted by an *asterisk* ($p < 0.05$). *n. s.*, not significant.

M2 receptors with carbachol elicited 2–3-fold higher TRPC4 and TRPC5 currents than activation of the M3 receptors. The TRPC4 and TRPC5 currents showed a typical doubly rectifying current-voltage relationship (Fig. 1, *A* and *E*). The stimulation of the M2 receptor increased both TRPC4 and TRPC5 currents in a dose-dependent manner (Fig. 1, *B* and *F*, *open column*, 1, 10, and 100 μM; $n = 5$, $n = 4$, $n = 12$, and $n = 4$, $n = 4$, $n = 10$), whereas the stimulation of the M3 receptor increased the TRPC4 current dose-dependently and the TRPC5 current dose-independently at the concentration range 1–100 μM carbachol (Fig. 1, *B* and *F*, *closed column*, 1, 10, and 100 μM; $n = 5$, $n = 8$, $n = 16$, and $n = 5$, $n = 7$, $n = 11$). Treatment with PTX markedly inhibited the TRPC4 and TRPC5 currents activated by M2 receptor stimulation and GTPγS (Fig. 1, *C*, *D*, *G*, and *H*; mock/PTX; $n = 8/n = 8$, $n = 5/n = 5$, $n = 7/n = 4$, and $n = 6/n = 3$). Thus, the M2 receptor-G$\alpha_{i/o}$ pathway was more effective than the M3 receptor-Gα_q pathway in channel activation by engaging the endogenous PTX-sensitive Gα proteins.

Specific Gα Isoforms Increase TPRC4 and TRPC5 Activity—To determine which Gα isoform is involved in the activation of TRPC4 and TRPC5, we used constitutively active forms of the Gα_i subunits (Gα QL mutants). Intracellular application of GTPγS through the patch pipette increased the TRPC4 current to 45.0 ± 7.2 pA/pF (Fig. 2*B*, mock, *closed column*, $n = 13$). The TRPC4 channel was activated to a different extent by all constitutively active G$\alpha_{i/o}$ subunits, even in the absence of GTPγS. Constitutively active Gα_{i3} and Gα_o mimicked the activation of TRPC4 by GTPγS (*open/closed column*, $n = 10/n = 8$ and $n = 9/n = 11$). Constitutively active Gα_{i1} activated the TRPC4 channel, whereas application of GTPγS significantly inhibited the TRPC4 current (*open/closed column*, $n = 13/n = 11$). Constitutively active Gα_{i2} (Gα_{i2}^{Q205L}) was the most effective activator among the Gα_i subunits tested (Fig. 2*B*, *open columns*, and supplemental Fig. S1*A*, $n = 6$). Notably, the application of GTPγS had no further effect on the TRPC4 current, indicating that Gα_{i2} fully activates TRPC4 (*closed column*, $n = 8$). Furthermore, stimulation of the M2 receptors (Fig. 1) and Gα_{i2} (Fig. 2) activated TRPC4 to the same extent. Of particular significance, constitutively active Gα_q was unable to activate TRPC4 (Fig. 2*B*, *open/closed column*, $n = 4/n = 3$). Moreover, constitutively active Gα_q inhibited the stimulatory effect of GTPγS. This was addressed further below.

Again, TRPC5 showed significant basal activity (36.6 ± 9.2 pA/pF, Fig. 2*C*, mock, *open column*). As with TRPC4, application of GTPγS further increased the TRPC5 current to 130.7 ± 16.7 pA/pF (Fig. 2*C*, mock, *closed column*, $n = 14$). Gα_{i3}^{Q205L} was the most effective activator of TRPC5, as all other Gα isoforms tested actually reduced the spontaneous current and GTPγS-induced currents, likely by competing with endogenous Gα_{i3} (Fig. 2*C* and supplemental Fig. S1*B*, *open/closed column*; Gα_{i1}, Gα_{i2}, Gα_{i3}, and Gα_o, $n = 12/n = 9$, $n = 6/n = 4$, $n = 7/n = 5$, and $n = 8/n = 9$). GTPγS did not increase the TRPC5

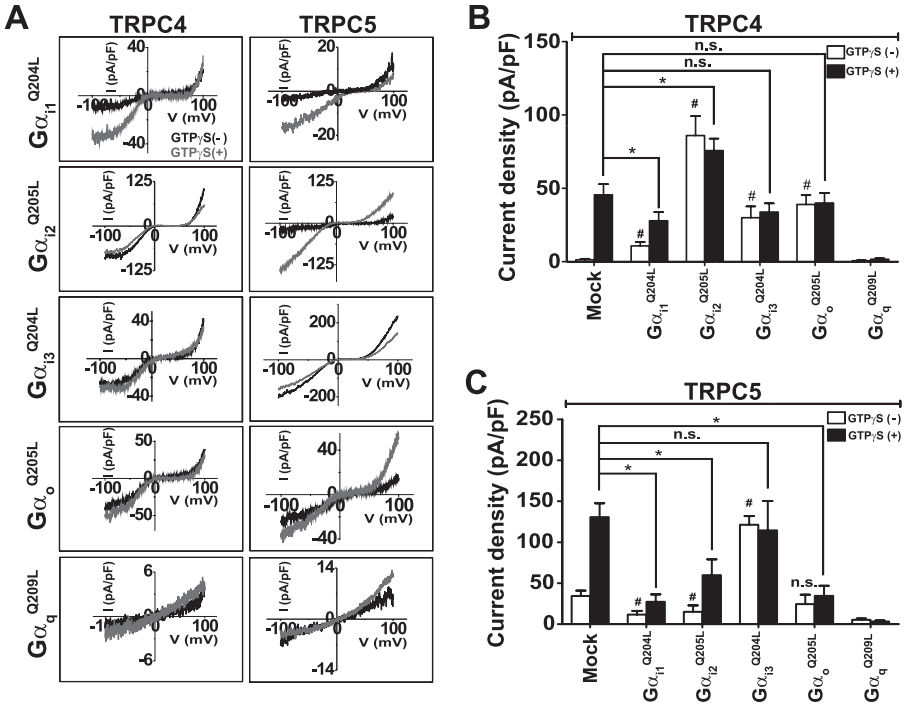

FIGURE 2. **Effect of Gα isoforms on TPRC4 and TRPC5 activity.** *A*, representative *I-V* relationships of TRPC4 and TRPC5 show the effect of constitutively active Gα QL mutants on the electrophysiological properties of the TRPC4 and TRPC5 channels. *B*, summary of TRPC4 current density activation by Gα subunits and/or by GTPγS. Note the variable effects of the Gα mutants. All Gα mutants activate TRPC4 channels without an activator (*e.g.* GTPγS or carbachol (*CCh*)). $G\alpha_{i2}$ provided the most effective activation of TRPC4, whereas $G\alpha_q$ inhibited TRPC4. Current density is represented by maximal current peaks (subtracted Cs^+ basal current) at −60 mV in Cs^+ solution and is indicated by means ± S.E. Statistical significance was denoted by an *asterisk* (*open column*) and *number sign* (*closed column*) at $p < 0.05$. *C*, summary of TRPC5 activation by Gα subtypes showing that the most effective activator is $G\alpha_{i3}$ and that most Gα mutants inhibit the TRPC5 channel, with $G\alpha_q$ inhibiting TRPC5. Current density was obtained by the methods described above. Statistical significance was denoted by an *asterisk* (*open column*) and *number sign* (*closed column*) at $p < 0.05$. *n. s.*, not significant.

current activated by $G\alpha_{i3}{}^{Q205L}$. As was found with TRPC4, constitutively active $G\alpha_q$ was not able to activate TRPC5 and instead inhibited the TRPC5 current (*open/closed column*, $n = 3/n = 3$).

Gβγ Isoforms Are Not Required for TPRC4 and TRPC5 Activation—Although $G\alpha_{i/o}$ subunits are key activators of TRPC4 or TRPC5, Gβγ subunits may also be involved in the activation of the channels, as is the case with GIRK channels, or in the regulation of the channels by altering the availability of activated $G\alpha_i$. To address these questions, we tested the effects of various Gβγ combinations on TRPC4 and TRPC5 activity. Figs. 3, *A–C* show that none of the Gβγ combinations tested activated the channels or reduced the activation by GTPγS. The exception is $G\beta_2\gamma_2$, which slightly inhibited the activation of TRPC5, likely by sequestering some of the $G\alpha_{i3}$ even in the presence of GTPγS. Moreover, even the free form $G\beta_1{}^{I80A}$ mutant (18, 20, 33, 34) did not activate TRPC4 or TRPC5 (Fig. 3*B*; *open/closed column*, $n = 4/n = 5$, and Fig. 3*C*; *open/closed column*; $n = 3/n = 14$). These results indicate that the PTX-sensitive $G\alpha_{i2/3}$ subunits are the activators of TRPC4 and TRPC5.

As is shown with the use of the Gβ mutant, $G\beta_1{}^{W99A}$, the major role of $G\beta_2\gamma_2$ in the activation of TRPC4 and TRPC5 is the sequestering of $G\alpha_{i/o}$ subunits. $G\beta_1{}^{W99A}$ keeps the G-protein as the heterotrimer $G\alpha\beta\gamma$ because $G\beta_1{}^{W99A}$ is unable to support nucleotide exchange on Gα (34). $G\beta_1{}^{W99A}$ inhibited activation of TRPC4 by M2 receptor stimulation to 61.4% ± 7.0% ($p = 0.03$, without/with $G\beta_1{}^{W99A}$, $n = 10/n = 12$), whereas $G\beta_1{}^{W99A}$ did not inhibit the modest M3-induced TRPC4 current (without/with $G\beta_1{}^{W99A}$, $n = 8/n = 10$). With TRPC5, $G\beta_1{}^{W99A}$ inhibited M2-induced TRPC5 current to 53.4% ± 16.7% ($p = 0.02$, without/with $G\beta_1{}^{W99A}$, $n = 11/n = 8$), without affecting the minimal M3-induced TRPC5 current (without/with $G\beta_1{}^{W99A}$, $n = 4/n = 6$, Fig. 3*D*). Importantly, $G\beta_1{}^{W99A}$ inhibited GTPγS-induced TRPC4 current to 46.2% ± 4.4% ($p = 0.00079$, without/with GTPγS, $n = 9/n = 8$) and GTPγS-induced TRPC5 current to 28.7% ± 7.7% ($p = 0.00075$, without/with GTPγS, $n = 6/n = 6$, Fig. 3*E*).

TRPC4 Is Inhibited by Increased $G\alpha_q$ Activity—Activation of the $G\alpha_q$-PLC pathway has been shown to modestly activate TRPC4 and TRPC5 (Fig. 1) by an unknown mechanism (1, 7, 8). Hence, the inhibition of TRPC4/5 by the constitutively active $G\alpha_q$ (Fig. 2) was completely unexpected. These results imply that intense overstimulation of a $G\alpha_q$-activated pathway inhibits TRPC4 and TRPC5. We considered several potential mechanisms, including increased or decreased cytoplasmic Ca^{2+}, interference of channel interaction with $G\alpha_i$, reduced surface expression of TRPC4, modified cellular PIP_2, and channel phosphorylation by PKC, known to induce desensitization of TRPC5 with phosphorylation of residue Thr-972 at the C terminus (35).

Loading the cells with BAPTA-AM recovered only 15 ± 5.6% (mock, 56.7 ± 11.2 pA/pF ($n = 6$); recovery by BAPTA, 9.8 ± 3.1 pA/pF; $n = 6$, BAPTA with GTPγS; $n = 12$, $G\alpha_q$ QL; $n = 3$, Fig. 4*A*), and inhibition of PKC with Goe6976 recovered only

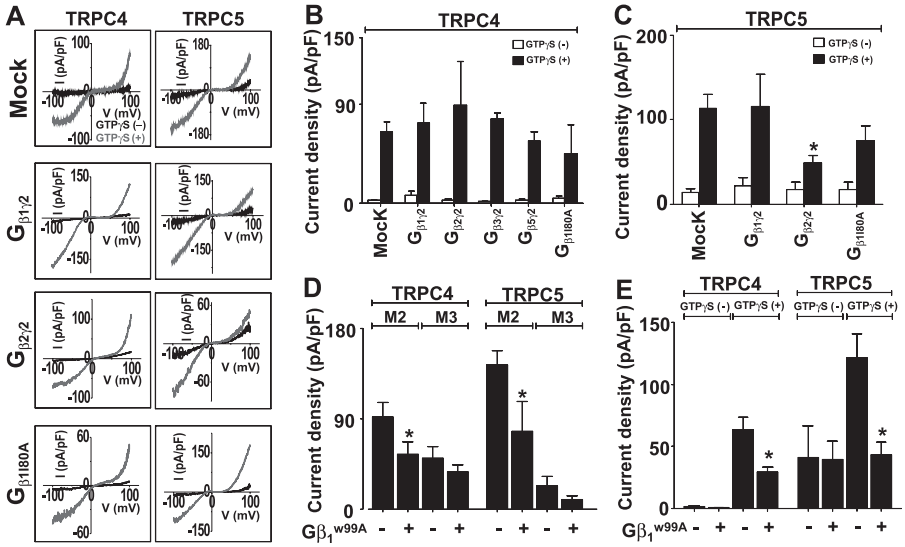

FIGURE 3. **Lack of effect of Gβγ isoforms on TPRC4 and TRPC5 activity.** *A* shows representative *I-V* curves of TRPC4 and TRPC5 co-expressed with or without the indicated Gβγ isoforms. *B* and *C* summarize the current density recorded in cells transfected with the indicated Gβγ subunits and infused with GTPγS (*closed columns*; mock, $G\beta_1\gamma_2$, $G\beta_2\gamma_2$, $G\beta_3\gamma_2$, and $G\beta_5\gamma_2$ with TRPC4; $n = 24$, $n = 5$, $n = 3$, $n = 7$, and $n = 7$; mock, $G\beta_1\gamma_2$, and $G\beta_2\gamma_2$ with TRPC5, $n = 10$, $n = 8$, and $n = 6$) or without (*open columns*; mock, $G\beta_1\gamma_2$, $G\beta_2\gamma_2$, $G\beta_3\gamma_2$, and $G\beta_5\gamma_2$ with TRPC4, $n = 15$, $n = 5$, $n = 4$, $n = 5$, and $n = 4$; mock, $G\beta_1\gamma_2$, and $G\beta_2\gamma_2$ with TRPC5, $n = 3$, $n = 5$, and $n = 3$). *D* shows the effects of $G\beta_1^{W99A}$ on activation of TRPC4 and TRPC5 by muscarinic receptors. The activation of TRPC4 and TRPC5 by the M2 receptor was inhibited by $G\beta_1^{W99A}$, whereas no current was activated by the M3 receptors. *E*, inhibition by $G\beta_1^{W99A}$ of TRPC4 and TRPC5 activated by GTPγS. All current densities represent maximal current peaks (subtracted Cs^+ basal current) at −60 mV in Cs^+ solution and are indicated by means ± S.E. Statistical significance was denoted by an *asterisk* ($p < 0.05$).

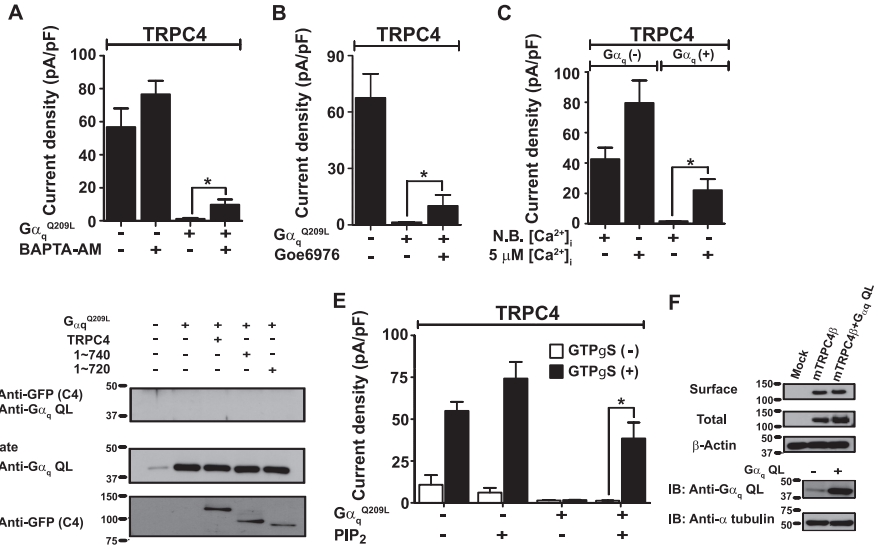

FIGURE 4. **Inhibition of TRPC4 by $G\alpha_q$ is rescued by PIP_2.** *A–C* show current densities in HEK293 cells stably expressing mTRPC4β and its inhibition by $G\alpha_q$. Loading the cells with BAPTA-AM and inhibition of PKC with Goe6976 did not effectively reverse channel inhibition by $G\alpha_q$. High intracellular Ca^{2+} (5 μM) reversed channel inhibition by $G\alpha_q$. *D*, TRPC4 and C-terminal truncation TRPC4 mutants did not co-IP with $G\alpha_q$. *E*, intracellular application of diC8-PIP_2 (50 μM) almost recovered the inhibition of TRPC4 by $G\alpha_q$. All current densities represent subtracted maximal current peaks at −60 mV in Cs^+ solution and are indicated by means ± S.E. Statistical significance was denoted by an *asterisk* ($p < 0.05$). All whole-cell currents were recorded in the intracellular application of GTPγS. *F*, surface expression of TRPC4 and $G\alpha_q$ co-expressed TRPC4 in HEK cells. Surface expression of TRPC4 was not altered by $G\alpha_q$ QL as determined by co-expression and surface biotinylation. Immunoblots of surface and total were detected by anti-GFP antibody (*upper panel*). Expression of endogenous $G\alpha_q$ and transfected $G\alpha_q$ QL were detected by Gαq antibody (*bottom panel*). *IB*, immunoblot. *N. B.*, non buffered.

13 ± 8.7% (mock, 67.6 ± 12.6 pA/pF ($n = 5$); recovery by PKC inhibitor, 10.1 ± 5.8 pA/pF ($n = 8$); $G\alpha_q$ QL ($n = 3$) Fig. 4*B*) of the TRPC4 current inhibited by $G\alpha_q$. The $G\alpha_q$-TRPC4-inhibited current was recovered to only 27.7 ± 9.2% by 5 μM intracellular Ca^{2+} (without $G\alpha_q^{Q209L}$, non-buffered/5 μM, $n = 7/n = 3$; with $G\alpha_q^{Q209L}$, non-buffered/5 μM, $n = 3/n = 3$; Fig. 4*C*). Co-IP experiments showed that TRPC4 does not interact directly with $G\alpha_q$ (Fig. 4*D*). Finally, activated $G\alpha_q$ did not change the surface expression of TRPC4 (Fig. 4*F*, *upper blots*). These findings rule out the effects of changes in cytosolic Ca^{2+}, PKC, and altered interaction with $G\alpha_i$ in channel inhibition by $G\alpha_q$ as the major inhibitors of the current induced by activated $G\alpha_q$. Moreover, they point to an indirect effect of $G\alpha_q$ on channel function.

$G\alpha_q$ activates PLC to hydrolyze PIP_2, reported to have an effect of TRPC4 and TRPC5 channel activity (7, 8). When diC8-PIP_2 (50 μM) was applied via the patch pipette together with GTPγS, it recovered $G\alpha_q$-induced inhibition of TRPC4 up to

51.83 ± 12.83% of the PIP_2 control (open/closed column, mock, PIP_2 alone, $G\alpha_q^{Q209L}$, and PIP_2 with $G\alpha_q^{Q209L}$; $n = 18/26$, $n = 4/15$, $n = 3/18$, and $n = 3/14$, Fig. 4*E*). PIP_2 was reported to inhibit TRPC4α but not the TRPC4β isoform (8), the isoform used in the present work. In addition, we reported that PIP_2 slows TRPC5 desensitization (7). Thus, the combined results in Fig. 4 indicate that PIP_2 and perhaps increased cytoplasmic Ca^{2+} are required for TRPC4 and TRPC5 activation.

Mechanisms Associated with Interaction between Gα$_{i2}$ with C Terminus of TRPC4—Together, the results in Figs. 1–4 indicate that activation of $G\alpha_i$ subunits by GPCRs is the primary mechanism for activating TRPC4 and TRPC5. This raised the question of whether activation of the channels requires direct interaction with the $G\alpha_i$ subunits, as was shown for other channels regulated by Gα (36) and Gβγ (33, 37) subunits. To address this question, we identified the TRPC4 and TRPC5 domain that might interact with the $G\alpha_i$ subunits. To characterize the association between TRPC4β with $G\alpha_{i2}$ *in vivo*, HEK cells were transfected with TRPC4β-GFP and $G\alpha_{i2}$, and their association was analyzed by co-immunoprecipitation. Immunoprecipitation of $G\alpha_{i2}$ pulled down TRPC4β-GFP (Fig. 5*A*, *upper panel*). Likewise, $G\alpha_{i2}$ was present in TRPC4β-GFP immunoprecipitates (Fig. 5*A*, *lower panel*). Similar co-immunoprecipitation occurred between TRPC5 and $G\alpha_{i3}$ (supplemental Fig. S2*A*). Pulldown assays were utilized to examine the binding of purified $G\alpha_{i2}^{Q205L}$ to GST fusion protein containing the C-terminal domain of TRPC4. $G\alpha_{i2}^{Q205L}$ bound to the C-terminal domain of TRPC4 (Fig. 5*A*, *right panel*).

To map the $G\alpha_{i2}$ binding domain in TRPC4β, a series of TRPC4β-GFP truncation or deletion mutants were generated (Fig. 5*B*). Binding domains for regulatory molecules are clustered in the C-terminal region of TRPC4 and TRPC5. Because considerable evidence suggests that modulation of TRPC4 and TRPC5 function are directed by elements present in this region, we focused on the C-terminal region. We made deletion mutants based on well known binding domains: the CIRB (calmodulin and inositol 1,4,5-trisphosphate receptor binding region) (amino acids 695–724), the SESTD1 (SEC14-like and spectrin-type domain 1) (amino acids 700–728), and the α-spectrin binding domain (amino acids 730–758). Of the truncations shown in Fig. 5*C*, Δ759–870 and Δ730–758 retained activation by $G\alpha_{i2}^{Q205L}$ with peak current amplitude similar to that of WT-TRPC4, although TRPC4 (Δ730–758) lost activation by GTPγS (open/closed column, mock, Δ695–724, Δ700–728, Δ730–758, and Δ759–870; $n = 8/7$, $n = 3/5$, $n = 3/4$, and $n = 9/6$; Fig. 5*C*). These results implicate amino acids upstream of 730 in channel activation by $G\alpha_i$. To further narrow the functional site, we examined the function of the 11 deletion or truncation TRPC4 mutants listed in Fig. 5*D*. $G\alpha_{i2}^{Q205L}$ did not activate TRPC4β-GFP 1–700, Δ700–710, Δ710–720, Δ700–740, Δ700–870, and Δ720–870, but fully or partially activated the other mutants with the typical doubly rectifying *I-V* curve (*open/closed column*, mock, Δ700–710, Δ710–720, Δ700–740, Δ720–730, Δ720–740, Δ720–870, Δ700–870, 1–760, 1–740, 1–720, and 1–700; $n = 27/12$, $n = 3/4$, $n = 3/3$, $n = 3/3$, $n = 10/10$, $n = 9/7$, $n = 3/5$, $n = 3/3$, $n = 8/9$, $n = 10/6$, $n = 5/8$, and $n = 3/4$; Fig. 5*E* and supplemental Fig. S3). Similarly, $G\alpha_{i3}^{Q205L}$ did not activate TRPC5-GFP Δ701–733, Δ707–717, Δ707–727, Δ707–735, Δ707–747, and Δ707–954, but fully or partially activated Δ737–765 and Δ764–954 (*open/closed column*, mock, Δ701–733, Δ707–747, Δ707–954, Δ737–765, and Δ764–954; $n = 12/12$, $n = 3/5$, $n = 3/3$, $n = 3/3$, $n = 3/3$, $n = 7/3$, $n = 3/3$, $n = 3/13$, and $n = 11/7$; supplemental Fig. S2).

The TRPC4β-GFP constructs were also co-expressed with $G\alpha_{i2}$ in HEK cells, and their interaction was monitored by co-immunoprecipitation. C-terminal (TRPC4β(1–720) and (1–740) truncations and TRPC4 (Δ721~740 and Δ759~870) deletions did not affect binding to $G\alpha_{i2}$, whereas deletion of the SESTD1 binding domain (Δ700~728) or of Δ700~870 eliminated association with $G\alpha_{i2}$ (Fig. 5*F*). Thus, the $G\alpha_{i2}$ binding domain maps to amino acids 700~728, the SESTD1 domain of TRPC4β.

To further analyze the interaction between the TRPC4 C terminus and $G\alpha_i$, we prepared C-terminal fragments of TRPC4 and examined their interactions with $G\alpha_i$. TRPC4β(621-700) did not interact with $G\alpha_i$, but TRPC4 fragments 621–720, 621–740, and 621–760 did (Fig. 5*G*), strengthening the conclusion that TRPC4(701–720) mediates the interaction with $G\alpha_{i2}$. The TRPC4(701–720) encompass the CaM and IP_3R binding region (10) (supplemental Fig. S4). The modeling in Fig. 6*A* of the interaction between $G\alpha_{i2}$ and TRPC4 suggested that the ^{711}RNLVKR^{716} region is important for binding, and thus, we prepared the mutants R711A, N712R, K715A, and R716A (Fig. 6 and supplemental Fig. S5). Of these mutants, K715A and R716A retained activation by $G\alpha_{i2}^{Q205L}$ with peak current amplitude similar to that of WT-TRPC4, whereas R711A and N712R lost partial or complete activation by both $G\alpha_{i2}^{Q205L}$ and GTPγS. However, the double mutant K715A/R716A did not respond to $G\alpha_{i2}^{Q205L}$ but maintained responsivity to GTPγS (*open/closed column*, mock, R711K, R711A, N712R, K715A, R716A, and K715A/R716A; $n = 6/11$, $n = 3/3$, $n = 15/3$, $n = 3/3$, $n = 3/9$, $n = 7/8$, and $n = 6/6$, Fig. 6*B*). These results implicate amino acids Lys-715 and Arg-716 in channel activation by $G\alpha_i$. Ordaz *et al.* (11) showed that a similar sequence in mTRPC5 (^{718}RNLVKR^{723}) is involved in the activation process by calmodulin (11). Thus, we used the mTRPC5 CIRBm1 (R718A/K722A/R723A), CIRBm2 (I717D/L720E/V721 A), and CBII mutants (ΔPro-828~Asn-854) (11) to test properties of TRPC5 activation by $G\alpha_{i3}$ (*open/closed column*, mock, CIRBm1, CIRBm2, and CBII: $n = 7/6$, $n = 4/6$, $n = 4/5$, and $n = 4/3$ in absence of $G\alpha_{i3}$; supplemental Fig. S6). The constitutively active $G\alpha_{i3}$ mutant could not activate the CIRBm1 and CIRBm2 deletion mutants but did activate the CBII mutant (*open/closed column*, mock, CIRBm1, CIRBm2, and CBII; $n = 6/6$, $n = 5/3$, $n = 4/4$, and $n = 6/4$; supplemental Fig. S6). Interaction between $G\alpha_i$ and the TRPC channels can also be demonstrated *in vivo*, as revealed by co-IP of TRPC4 with $G\alpha_{i2}$ and of TRPC5 with $G\alpha_{i3}$ in brain extract (Fig. 5*H*).

DISCUSSION

We report here that the primary mechanism for the activation of TRPC4 and TRPC5 in gastric smooth muscle *in vivo* is through activation of GPCR. TRPC4 and TRPC5 activation appears to require both M2-$G_{i/o}$ and M3-$G_{q/11}$ muscarinic receptors (20). The mechanism involves specific activation of

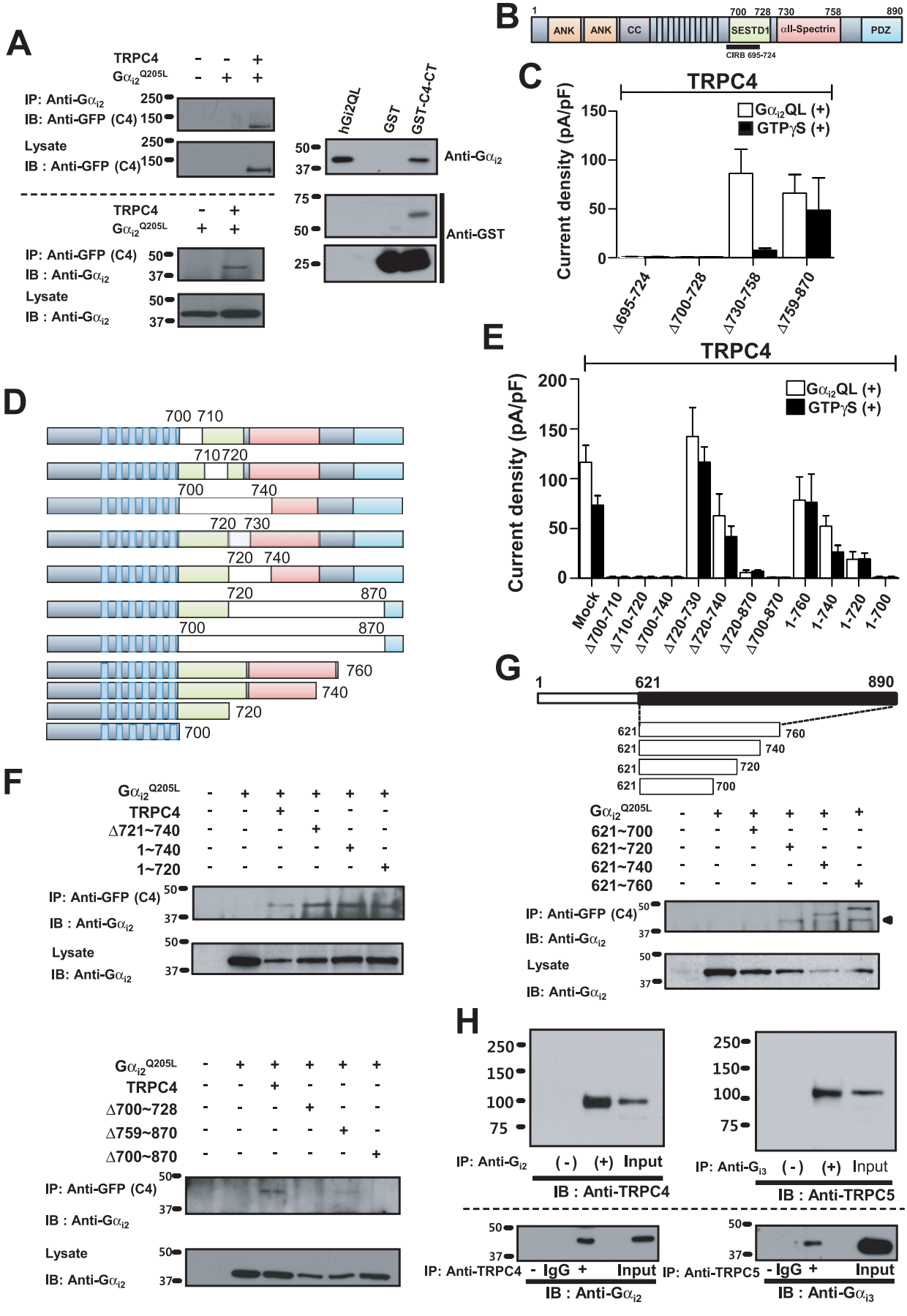
A
TRPC4
Gαi2Q205L
IP: Anti-Gαi2
IB: Anti-GFP (C4)
Lysate
IB : Anti-GFP (C4)
hGi2QL
GST
GST-C4-CT
Anti-Gαi2
Anti-GST
IP: Anti-GFP (C4)
IB : Anti-Gαi2
B
ANK
CC
SESTD1
αII-Spectrin
PDZ
CIRB 695-724
C
TRPC4
Gαi2QL (+)
GTPγS (+)
Current density (pA/pF)
Δ695-724
Δ700-728
Δ730-758
Δ759-870
D
E
TRPC4
Mock
Δ700-710
Δ710-720
Δ700-740
Δ720-730
Δ720-740
Δ720-870
Δ700-870
1-760
1-740
1-720
1-700
F
TRPC4
Δ721~740
1~740
1~720
Δ700~728
Δ759~870
Δ700~870
G
621~700
621~720
621~740
621~760
H
IP: Anti-Gi2
IP: Anti-Gi3
IB : Anti-TRPC4
IB : Anti-TRPC5
IP: Anti-TRPC4
IP: Anti-TRPC5
IgG
Input
IB : Anti-Gαi2
IB : Anti-Gαi3

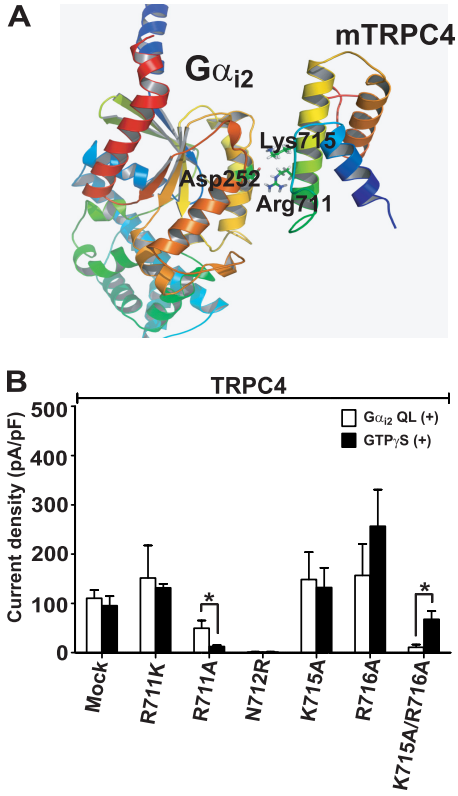

FIGURE 6. **The interaction modeling of the TRPC4 C terminus (amino acids 701–720) with Gα$_{i2}$.** *A*, a model of association between Gα$_{i2}$ and TRPC4. An ionic interaction was assumed between the two proteins. Amino acids from 671 to 758 of TRPC4 are shown. *B*, summary of effects of Gα$_{i2}^{Q205L}$ on current by mTRPC4 and mTRPC4 mutants in the presence and absence of GTPγS stimulation. mTRPC4 mutants were substituted at CIRB residues (R711K, R711A, N712R, K715A, and R716A). All current densities represent maximal current peaks (subtracted Cs^+ basal current) at −60 mV in Cs^+ solution and are indicated by means ± S.E. Statistical significance was denoted by an *asterisk* ($p < 0.05$).

the channels by Gα$_i$ subunits. Receptors coupled to Gα$_{i2}$ primarily activate TRPC4 and receptors coupled to Gα$_{i3}$ primarily activate TRPC5 to mediate the receptor-stimulated monovalent cation current and the Ca^{2+} influx.

Several studies have reported modulation of TRPC4 and TRPC5 activity by GTPγS-activated PTX-sensitive G-proteins and G$_{i/o}$-coupled receptors (6, 8, 25). Activation of TRPC4 by muscarinic receptor stimulation of GI smooth muscle was inhibited by PTX and was shown to be critical in evoking and regulating GI tract motility (21). Our results provide a molecular mechanism to explain the activation of TRPC4 by the PTX-sensitive G-protein signaling. A unique feature of the mI_{CAT} is that it requires simultaneous activation of both the M2 and M3 muscarinic receptors. Conversely, cationic channel activation in murine gut smooth muscle cells involves three separate pathways (24). 1) The M3-Gα$_q$-PLCβ system, which transiently activates the 70-pS and 120-pS cationic channels concurrently with inositol 1,4,5-trisphosphate-induced Ca^{2+} release. 2) The M2 pathway, which transduces signals from M2 receptors via Gα$_o$ to the 70-pS cationic channel and shifts the transient activation toward a longer open mode. 3) The M2/M3 pathway, which transmits M2 signals via Gα$_o$ and M3 signals via a Gα$_q$-independent PLC, to the 70-pS cationic channel, resulting in a much longer open mode. The latter pathway does not work well when either the M2 or the M3 receptors are lacking or when either Gα$_o$ or PLC are inactivated. In addition, the M2/M3 pathway, but not the M2 or M3 pathway, involves processes in which Ca^{2+} has a potentiating effect on channel activation, suggesting that the M3 pathway may facilitate the function of the M2/M3 pathway through inositol 1,4,5-trisphosphate-induced Ca^{2+} release (38). We argue that if the 70-pS channel is mediated by TRPC4, then the pathways involving the M2 receptors use Gα$_{i2}$ to directly activate the channel.

In addition to TRPC4/5, activation by the Gα$_{i/o}$ subunits have been reported to regulate several other TRP channels. For example, in G$_o$-coupled mGluR6, Gα$_o$ closes a downstream nonselective cation channel in ON bipolar cells that is mediated by TRPM1-L (39). Pheromone sensing in the vomeronasal organ is mediated by V1R-G$_i$ and V2R-G$_o$ complexes that activate TRPC2 (40). Whether activation of these channels is by direct interaction with Gα$_{i/o}$ subunits as shown here for TRPC4/TRPC5 remains to be determined.

Our findings indicate that regulation of TRPC4 and TRPC5 by G-proteins is more complex than assumed previously. The newly discovered mechanism for activation of TRPC4 and TRPC5 suggests that Ca^{2+} influx through these channels can be activated by several mediators depending on receptor stimulation. As reported before and shown in Fig. 1, TRPC4 and TRPC5 can clearly be activated by Gα$_q$-coupled receptors and mediated by several of the mechanisms reported before. However, activation by Gα$_q$-coupled receptors appears to be modest (Fig. 1). More significant activation of TRPC4/5 is elicited by stimulation of Gα$_i$-coupled receptors that is mediated by direct activation of the channels by Gα$_i$ subunits. The Gα$_i$ binding domain in TRPC4 and TRPC5 shares binding motifs with other regulatory molecules (CIRB, SESTD1) in the C-terminal region of TRPC4 and TRPC5. Modeling and mutation analyses indicate that the ^{711}RNLVKR^{716} region is important for the interaction between Gα$_{i2}$ and TRPC4 (supplemental Fig. S6). By contrast with GIRK channels, Gβγ subunits do not appear to be involved in the direct activation of TRPC4 or TRPC5 by Gα$_i$. It

FIGURE 5. **Interaction of Gα$_{i2}$ with the C terminus of TRPC4.** *A*, TRPC4 co-immunoprecipitates with Gα$_{i2}$. HEK cells were transfected with empty vector, Gα$_{i2}$ alone, and Gα$_{i2}$ with TRPC4-GFP and were used to test reciprocal co-IP of TRPC4 and Gα$_{i2}$. TRPC4 C-terminal GST fusion protein was used to probe direct binding between Gα$_{i2}$ and TRPC4. Binding of the TRPC4 C-terminal GST fusion protein with recombinant human Gαi2^{Q205L} protein was shown by Gα$_{i2}$-antibody *in vitro* binding assay. *B*, a schematic of GFP-fused TRPC4. *C*, summary of the effects of Gα$_{i2}$ on TRPC4 C-terminal truncation mutants in the presence and absence of GTPγS stimulation. Current densities are represented by subtracted maximal maximal current peaks at −60 mV in Cs^+ solution and are indicated by means ± S.E. *D*, schematic of GFP-fused TRPC4 deletion and truncation mutants used (*upper panel*). Wild-type TRPC4 and mutants were probed using the GFP antibody in immunoblotting (*bottom*). *E*, summary of the effects of Gα$_{i2}$ on current by TRPC4 deletion and truncation mutants in the presence and absence of GTPγS stimulation. Current density was obtained by the methods described above. *F*, interaction between Gα$_{i2}$, TRPC4, and mutants was tested by co-IP, and the interaction site was mapped to the 700∼728 region (the SESTD1 domain of TRPC4β). *G*, a schematic of GFP-fused C-terminal fragments of TRPC4 (*upper panel*) and their co-IP with Gα$_{i2}$. *H*, the association between Gα$_i$ with TRPC4/5 *in vivo*. Gα$_{i2}$ and Gα$_{i3}$ were immunoprecipitated from rat brain extract and were probed for TRPC4 and TRPC5 to show co-IP *in vivo* (*upper panel*). TRPC4 and TRPC5 were co-immunoprecipitated reciprocally. Lanes of IgG and control (−) did not show Gα$_i$ binding. *Input* was indicated as 10% input of brain extract. *IB*, immunoblot.

is likely that the major role of $G\beta\gamma$ is regulating channel function by sequestering $G\alpha_{i/o}$ subunits in the resting state. The mode of TRPC4/TRPC5 regulation by $G\alpha_{i/o}$ subunits reported here likely constitutes a major pathway in smooth muscle. It will be interesting to explore the full potential of this form of regulation in other cell types, particularly when the regulation by $G\alpha_{i/o}$-coupled receptors involves changes in cellular Ca^{2+}. Examples include acetylcholine-induced vasoregulation, lung microvascular permeability (41, 42) and the increase of 5-hydroxytryptamine 2 receptor-coupled GABA release in thalamic interneurons (43). In summary, the present findings expand knowledge regarding signal transduction by cytoplasmic Ca^{2+} beyond the $G\beta\gamma$ to the $G\alpha$ subunits of $G\alpha_i$-coupled receptors. Moreover, our findings point to a signaling function that is activated rather than inhibited by $G\alpha_i$ proteins and add an important function to the repertoire of functions activated by $G\alpha_i$ subunits.

Acknowledgments—We thank Dr. Yong-Sung Juhnn for the human $G\alpha_{i1}^{Q204L}$, $G\alpha_{i3}^{Q204L}$, rat $G\alpha_{i2}^{Q205L}$, and human $G\alpha_q^{Q209L}$; Dr. Seong-Woo Jeong for all the $G\beta\gamma$; Dr. Michel X. Zhu for the mTRPC5 and CIRB mutants; and Dr. Yasuo Mori for the mTRPC5-GFP and ΔC.

REFERENCES

1. Schaefer, M., Plant, T. D., Obukhov, A. G., Hofmann, T., Gudermann, T., and Schultz, G. (2000) Receptor-mediated regulation of the nonselective cation channels TRPC4 and TRPC5. *J. Biol. Chem.* **275,** 17517–17526
2. Miehe, S., Bieberstein, A., Arnould, I., Ihdene, O., Rütten, H., and Strübing, C. (2010) The phospholipid-binding protein SESTD1 is a novel regulator of the transient receptor potential channels TRPC4 and TRPC5. *J. Biol. Chem.* **285,** 12426–12434
3. Blair, N. T., Kaczmarek, J. S., and Clapham, D. E. (2009) Intracellular calcium strongly potentiates agonist-activated TRPC5 channels. *J. Gen. Physiol.* **133,** 525–546
4. Gross, S. A., Guzmán, G. A., Wissenbach, U., Philipp, S. E., Zhu M. X., Bruns, D., and Cavalié, A. (2009) TRPC5 is a Ca^{2+}-activated channel functionally coupled to Ca^{2+}-selective ion channels. *J. Biol. Chem.* **284,** 34423–34432
5. Flemming, P. K., Dedman, A. M., Xu, S. Z., Li, J., Zeng, F., Naylor, J., Benham, C. D., Bateson, A. N., Muraki, K., and Beech, D. J. (2006) Sensing of lysophospholipids by TRPC5 calcium channel. *J. Biol. Chem.* **281,** 4977–4982
6. Xu, S. Z., Muraki K., Zeng F., Li J., Sukumar P., Shah S., Dedman, A. M., Flemming, P. K., McHugh, D., Naylor, J., Cheong, A., Bateson, A. N., Munsch C. M., Porter, K. E., and Beech, D. J. (2006) A sphingosine 1-phosphate-activated calcium channel controlling vascular smooth muscle cell motility. *Circ. Res.* **98,** 1381–1389
7. Kim, B. J., Kim, M. T., Jeon, J. H., Kim, S. J., and So, I. (2008) Involvement of phosphatidylinositol 4,5-bisphosphate in the desensitization of canonical transient receptor potential 5. *Biol. Pharm. Bull.* **31,** 1733–1738
8. Otsuguro, K., Tang, J., Tang, Y., Xiao, R., Freichel, M., Tsvilovskyy, V., Ito, S., Flockerzi, V., Zhu, M. X., and Zholos, A. V. (2008) Isoform-specific inhibition of TRPC4 channel by phosphatidylinositol 4,5-bisphosphate. *J. Biol. Chem.* **283,** 10026–10036
9. Trebak, M., Lemonnier, L., DeHaven, W. I., Wedel, B. J., Bird, G. S., and Putney, J. W., Jr. (2009) Complex functions of phosphatidylinositol 4,5-bisphosphate in regulation of TRPC5 cation channels. *Pflugers Arch.* **457,** 757–769
10. Tang, J., Lin, Y., Zhang, Z., Tikunova, S., Birnbaumer, L., and Zhu, M. X. (2001) Identification of common binding sites for calmodulin and inositol 1,4,5-trisphosphate receptors on the carboxyl termini of trp channels. *J. Biol. Chem.* **276,** 21303–21310
11. Ordaz, B., Tang, J., Xiao, R., Salgado, A., Sampieri, A., Zhu, M. X., and Vaca, L. (2005) Calmodulin and calcium interplay in the modulation of TRPC5 channel activity. Identification of a novel C-terminal domain for calcium/calmodulin-mediated facilitation. *J. Biol. Chem.* **280,** 30788–30796
12. Shi, J., Mori, E., Mori, Y., Mori, M., Li, J., Ito, Y., and Inoue, R. (2004) Multiple regulation by calcium of murine homologues of transient receptor potential proteins TRPC6 and TRPC7 expressed in HEK293 cells. *J. Physiol.* **561,** 415–432
13. Kim, M. T., Kim, B. J., Lee, J. H., Kwon, S. C., Yeon, D. S., Yang, D. K., So, I., and Kim, K. W. (2006) Involvement of calmodulin and myosin light chain kinase in activation of mTRPC5 expressed in HEK cells. *Am. J. Physiol. Cell Physiol.* **290,** C1031–1040
14. Kim, B. J., Jeon, J. H., Kim, S. J., and So, I. (2007) Role of calmodulin and myosin light chain kinase in the activation of carbachol-activated cationic current in murine ileal myocytes. *Can. J. Physiol. Pharmacol.* **85,** 1254–1262
15. Shimizu, S., Yoshida, T., Wakamori, M., Ishii, M., Okada, T., Takahashi, M., Seto, M., Sakurada, K., Kiuchi, Y., and Mori, Y. (2006) Ca^{2+}-calmodulin-dependent myosin light chain kinase is essential for activation of TRPC5 channels expressed in HEK293 cells. *J. Physiol.* **570,** 219–235
16. Bezzerides, V. J., Ramsey, I. S., Kotecha, S., Greka, A., and Clapham, D. E. (2004) Rapid vesicular translocation and insertion of TRP channels. *Nat. Cell Biol.* **6,** 709–720
17. Xu, S. Z., Sukumar, P., Zeng, F., Li, J., Jairaman, A., English, A., Naylor, J., Ciurtin, C., Majeed, Y., Milligan, C. J., Bahnasi, Y. M., Al-Shawaf, E., Porter, K. E., Jiang, L. H., Emery, P., Sivaprasadarao, A.,and Beech, D. J. (2008) TRPC channel activation by extracellular thioredoxin. *Nature* **451,** 69–72
18. Yoshida, T., Inoue, R., Morii, T., Takahashi N., Yamamoto S., Hara Y., Tominaga M., Shimizu S., Sato Y., and Mori, Y. (2006) Nitric oxide activates TRP channels by cysteine *S*-nitrosylation. *Nat. Chem. Biol.* **2,** 596–607
19. So, I., and Kim, K. W. (2003) Nonselective cation channels activated by the stimulation of muscarinic receptors in mammalian gastric smooth muscle. *J. Smooth Muscle Res.* **39,** 231–247
20. Lee, K. P., Jun, J. Y., Chang, I. Y., Suh, S. H., So, I., and Kim, K. W. (2005) TRPC4 is an essential component of the nonselective cation channel activated by muscarinic stimulation in mouse visceral smooth muscle cells. *Mol. Cell* **20,** 435–441
21. Tsvilovskyy, V. V., Zholos, A. V., Aberle, T., Philipp, S. E., Dietrich, A., Zhu, M. X., Birnbaumer, L., Freichel, M., and Flockerzi, V. (2009) Deletion of TRPC4 and TRPC6 in mice impairs smooth muscle contraction and intestinal motility *in vivo*. *Gastroenterology* **137,** 1415–1424
22. Kim, Y. C., Kim, S. J., Sim, J. H., Cho, C. H., Juhnn, Y. S., Suh, S. H., So, I., and Kim, K. W. (1998) Suppression of the carbachol-activated nonselective cationic current by antibody against α subunit of Go protein in guinea pig gastric myocytes. *Pflugers Arch.* **436,** 494–496
23. Yan, H. D., Okamoto, H., Unno, T., Tsytsyura, Y. D., Prestwich, S. A., Komori, S., Zholos, A. V., and Bolton, T. B. (2003) Effects of G-protein-specific antibodies and G $\beta\gamma$ subunits on the muscarinic receptor-operated cation current in guinea pig ileal smooth muscle cells. *Br. J. Pharmacol.* **139,** 605–615
24. Sakamoto, T., Unno, T., Kitazawa, T., Taneike, T., Yamada, M., Wess, J., Nishimura, M., and Komori, S. (2007) Three distinct muscarinic signaling pathways for cationic channel activation in mouse gut smooth muscle cells. *J. Physiol.* **582,** 41–61
25. Jeon, J. P., Lee, K. P., Park, E. J., Sung, T. S., Kim, B. J., Jeon, J. H., and So, I. (2008) The specific activation of TRPC4 by Gi protein subtype. *Biochem. Biophys. Res. Commun.* **377,** 538–543
26. Sung, T. S., Jeon, J. P., Kim, B. J., Hong, C., Kim, S. Y., Kim, J., Jeon, J. H., Kim, H. J., Suh, C. K., Kim, S. J., and So, I. (2011) Molecular determinants of PKA-dependent inhibition of TRPC5 channel. *Am. J. Physiol. Cell Physiol.* **301,** C823–832
27. Kim, M. J., Jeon, J. P., Kim, H. J., Kim, B. J., Lee, Y. M., Choe, H., Jeon, J. H., Kim, S. J., and So, I. (2008) Molecular determinant of sensing extracellular pH in classical transient receptor potential channel 5. *Biochem. Biophys. Res. Commun.* **365,** 239–245
28. Sali, A., and Blundell, T. L. (1993) Comparative protein modeling by sat-

isfaction of spatial restraints. *J. Mol. Biol.* **234,** 779–815
29. Roy, A., Kucukural, A., and Zhang, Y. (2010) I-TASSER: A unified platform for automated protein structure and function prediction. *Nat. Protoc.* **5,** 725–738
30. Zhang, Y. (2008) I-TASSER server for protein three-dimensional structure prediction. *BMC Bioinformatics* **9,** 40
31. Miller, M., Shi, J., Zhu, Y., Kustov, M., Tian, J. B., Stevens, A., Wu, M., Xu, J., Long, S., Yang, P., Zholos, A. V., Salovich, J. M., Weaver, C. D., Hopkins, C. R., Lindsley, C. W., McManus, O., Li M., and Zhu M. X. (2011) Identification of ML204, a novel potent antagonist that selectively modulates native TRPC4/C5 ion channels. *J. Biol. Chem.* **286,** 33436–33446
32. Sung, T. S., Kim, M. J., Hong, S., Jeon, J. P., Kim, B. J., Jeon, J. H., Kim, S. J., and So, I. (2009) Functional characteristics of TRPC4 channels expressed in HEK 293 cells. *Mol. Cells* **27,** 167–173
33. Ford, C. E., Skiba, N. P., Bae, H., Daaka, Y., Reuveny, E., Shekter, L. R., Rosal, R., Weng, G., Yang, C. S., Iyengar, R., Miller, R. J., Jan, L. Y., Lefkowitz, R. J., and Hamm, H. E. (1998) Molecular basis for interactions of G-protein $\beta\gamma$ subunits with effectors. *Science* **280,** 1271–1274
34. Riven, I., Iwanir, S., and Reuveny, E. (2006) GIRK channel activation involves a local rearrangement of a preformed G-protein channel complex. *Neuron* **51,** 561–573
35. Zhu, M. H., Chae, M., Kim, H. J., Lee, Y. M., Kim, M. J., Jin, N. G., Yang, D. K., So, I., and Kim, K. W. (2005) Desensitization of canonical transient receptor potential channel 5 by protein kinase C. *Am. J. Physiol. Cell Physiol.* **289,** C591–600
36. Clancy, S. M., Fowler, C. E., Finley, M., Suen, K. F., Arrabit, C., Berton, F., Kosaza, T., Casey, P. J., and Slesinger, P. A. (2005) Pertussis-toxin-sensitive $G\alpha$ subunits selectively bind to C-terminal domain of neuronal GIRK channels: Evidence for a heterotrimeric G-protein-channel complex. *Mol. Cell Neurosci.* **28,** 375–389
37. Finley, M., Arrabit, C., Fowler, C., Suen, K. F., and Slesinger, P. (2004) βL-βM loop in the C-terminal domain of G-protein-activated inwardly rectifying K^+ channels is important for $G\beta\gamma$ subunit activation. *J. Physiol.* **555,** 643–657
38. Zholos, A. V., and Bolton, T. B. (1997) Muscarinic receptor subtypes controlling the cationic current in guinea pig ileal smooth muscle. *Br. J. Pharmacol.* **122,** 885–893
39. Koike, C., Obara, T., Uriu, Y., Numata, T., Sanuki, R., Miyata, K., Koyasu, T., Ueno, S., Funabiki, K., Tani, A., Ueda, H., Kondo, M., Mori, Y., Tachibana, M., and Furukawa, T. (2010) TRPM1 is a component of the retinal ON bipolar cell transduction channel in the mGluR6 cascade. *Proc. Natl. Acad. Sci. U.S.A.* **107,** 332–337
40. Zhang, P., Yang, C., and Delay, R. J. (2010) Odors activate dual pathways, a TRPC2 and an AA-dependent pathway, in mouse vomeronasal neurons. *Am. J. Physiol. Cell Physiol.* **298,** C1253–1264
41. Freichel, M., Suh, S. H., Pfeifer, A., Schweig, U., Trost, C., Weissgerber, P., Biel, M., Philipp, S., Freise, D., Droogmans, G., Hofmann, F., Flockerzi, V., and Nilius, B. (2001) Lack of an endothelial store-operated Ca^{2+} current impairs agonist-dependent vasorelaxation in $TRP4^{-/-}$ mice. *Nat. Cell Biol.* **3,** 121–127
42. Tiruppathi, C., Freichel, M., Vogel, S. M., Paria, B. C., Mehta, D., Flockerzi, V., and Malik, A. B. (2002) Impairment of store-operated Ca^{2+} entry in $TRPC4^{-/-}$ mice interferes with increase in lung microvascular permeability. *Circ. Res.* **91,** 70–76
43. Munsch, T., Freichel, M., Flockerzi, V., and Pape, H. C. (2003) Contribution of transient receptor potential channels to the control of GABA release from dendrites. *Proc. Natl. Acad. Sci. U.S.A.* **100,** 16065–16070